






## Direct insulator to relativistic quantum Hall transition in graphene

Ching-Chen Yeh <sup>1,2</sup> Pin-Chi Liao,<sup>1,\*</sup> Dinesh K. Patel <sup>1,2,3</sup> Wei-Chen Lin <sup>4,5</sup> Siang-Chi Wang,<sup>1</sup>  
Albert F. Rigosi,<sup>2</sup> Randolph E. Elmquist <sup>2</sup> and Chi-Te Liang <sup>1,6,7,\*</sup>

<sup>1</sup>Department of Physics, National Taiwan University, Taipei 106, Taiwan

<sup>2</sup>Physical Measurement Laboratory, National Institute of Standards and Technology (NIST), Gaithersburg, Maryland 20899, USA

<sup>3</sup>Physikalisch-Technische Bundesanstalt (PTB) Bundesallee 100, Braunschweig 38116, Germany

<sup>4</sup>Taiwan International Graduate Program, Academia Sinica, Taipei 115, Taiwan

<sup>5</sup>Department of Engineering and System Science, National Tsing Hua University, Hsinchu 300, Taiwan

<sup>6</sup>Center for Quantum Science and Engineering, National Taiwan University, Taipei 106, Taiwan

<sup>7</sup>Taiwan Consortium of Emergent Crystalline Materials (TCECM), Taipei 106, Taiwan



(Received 26 July 2023; revised 7 October 2023; accepted 19 October 2023; published 13 November 2023)

We present evidence of the direct insulator-quantum Hall transition in monolayer epitaxial graphene, a genuine two-dimensional (2D) system. We studied the transition from an insulating state to a quantum Hall state at a high Landau level filling factor  $\nu = 6 > 3$  and the plateau-plateau transition from  $\nu = 6$  to  $\nu = 2$ . Using scaling theory, the critical exponent  $\kappa$  was determined to be  $0.41 \pm 0.02$  for the direct insulator-quantum Hall transition. This closely aligns with  $\kappa = 0.42 \pm 0.02$  from the  $\nu = 6$  to  $\nu = 2$  quantum Hall plateau-plateau transition. These findings suggest that the two transitions may belong to the same universality class. While similar transitions have been explored in conventional two-dimensional charge systems, our study provides valuable insights into a truly 2D system, deepening our understanding of these transitions.

DOI: [10.1103/PhysRevB.108.205304](https://doi.org/10.1103/PhysRevB.108.205304)

**Introduction.** The direct insulator-quantum Hall (I-QH) transition corresponds to a transition from an insulating state to a high Landau level (LL) filling factor ( $\nu \geq 3$ ) quantum Hall (QH) state [1]. Such a transition occurs when the Fermi energy crosses the  $N \geq 1$  LL (normally spin or/and valley degenerate) when a magnetic field is applied perpendicularly to the plane of a two-dimensional (2D) charge system. Although this transition cannot be explained by the global phase diagram (GPD) proposed by Kivelson, Lee, and Zhang, which predicts that the I-QH transition only occurs when the Fermi level crosses the  $N = 0$  LL [2–5], studies on the direct I-QH transition in a variety of quasi-2D systems have been reported [1,6–15]. However, research on the direct I-QH transition in monolayer graphene, which is a truly 2D system, is still lacking [16,17].

Similar to the direct I-QH transition, another magnetic-field-induced transition related to the quantum Hall effect, the QH plateau-plateau (P-P) transition has been extensively studied for more than 30 years [18–27] and is well established in the field of QH physics. In the pioneering work done by Wei *et al.* [18], the finite-size scaling theory was developed to investigate the critical behavior in the P-P transition, and the critical exponent  $\kappa$  was measured to be  $0.42 \pm 0.04$  for a spin-split P-P transition by analyzing the maximum of  $d\rho_{xy}/dB \sim T^{-\kappa}$  at different temperatures [18,19], where  $\rho_{xy}$ ,  $B$ , and  $T$  represent the Hall resistivity, external applied magnetic field, and temperature, respectively. It should be noted that  $\kappa$  depends on spin/valley degeneracy, and for a spin-degenerate P-P tran-

sition,  $\kappa$  was measured to be  $0.21 \pm 0.02$  [20]. Furthermore, some studies have explored the P-P transition in graphene, and determined the value  $\kappa \approx 0.42$  [23,25] which has been interpreted to be consistent with the finding of Wei *et al.* [18], even though both spin and valley degeneracies in their graphene devices need to be considered [23,25]. Notably, it is important to acknowledge that the relativistic nature of Dirac fermions in monolayer graphene leads to the observation of the anomalous integer QH effect, where  $\sigma_{xy} = (n + 1/2)(4e^2/h)$  with  $n = 0, 1, 2, \dots$ . Here the number 4 corresponds to fourfold (spin and valley) degeneracy. Additionally, the measured critical exponents in different 2D systems span a wide range of values ( $0.15 \leq \kappa \leq 0.81$ ) [18,24,28–35], and it has been argued that the value of  $\kappa$  for the P-P transition may not be universal [24].

In this study, we provide experimental evidence for a direct I-QH transition in monolayer graphene. While this transition has been observed in other systems, it is worth noting that our study brings forth insights into a truly 2D system. This transition from an insulator to a  $\nu = 6$  quantum Hall state was characterized, and by examining  $|d\rho_{xx}/dB|$  near the critical magnetic field  $B_c$ , the critical exponent  $\kappa$  was found to be  $0.41 \pm 0.02$ . This aligns with the value  $\kappa \approx 0.42 \pm 0.02$  from the  $\nu = 6$  to  $\nu = 2$  P-P transition, suggesting that both transitions could be of the same universality class.

**Experimental results.** Our experiments were performed on monolayer epitaxial graphene which was grown on a semi-insulating 4H-SiC(0001) substrate. The graphene sample was patterned into a Hall bar geometry with dimensions of 2000  $\mu\text{m}$  in length and 400  $\mu\text{m}$  in width, employing standard lithography and etching techniques. To improve the contact resistance, superconducting NbTiN contact pads were deposited onto the graphene [36]. These contact pads enhance

\*Corresponding authors: f08222043@g.ntu.edu.tw;  
ctliang@phys.ntu.edu.tw

the electrical contact and minimize resistance, allowing for more accurate transport measurements. At the end of the fabrication process, in order to stabilize the long-term electrical properties of the device [37] and introduce disorder which is necessary for observing the direct I-QH transition, the graphene device was functionalized with chromium tricarbonyl [Cr(CO)<sub>3</sub>]. This functionalization process helps to maintain the device's electrical properties over an extended period of time and introduces the required disorder for the desired transition. The resulting device is a high-quality, tunable carrier-density graphene device that has been specifically developed for use in quantum Hall resistance standard array devices [37–41]. To vary the carrier density of our graphene device, we use low-temperature light illumination instead of using the vacuum gentle heating technique, which is suitable for a small-sample-space He<sup>4</sup> cryostat [37]. This device provides a reliable platform for investigating the direct I-QH transition and enables precise measurements of quantized Hall resistances [41]. More details about the device fabrication and characterization can be found in the Supplemental Material [42] (see also references [43–47] therein). The longitudinal resistivity  $\rho_{xx}$  and the Hall resistivity  $\rho_{xy}$  of our graphene device were measured simultaneously by using a standard low-frequency AC lock-in technique at a frequency of 13.1 Hz in a cryofree <sup>3</sup>He/<sup>4</sup>He dilution refrigerator at low temperatures.

According to the Onsager-Casimir relations [48–50], electrical conductance should exhibit symmetry when subjected to opposing magnetic field directions. However, our preliminary data indicated an unexpected degree of asymmetry, which we suspect might arise from the unintended mixing of  $\rho_{xx}$  with  $\rho_{xy}$ . To rectify this, we adopted a methodology that combined data from both positive and negative magnetic field directions, capitalizing on the inherent symmetries of the resistivity components. This strategy effectively mitigated the mixing issue as highlighted in prior research [51,52], enhancing the accuracy and consistency of our measurements. Figure 1 illustrates the symmetrized longitudinal resistivity and the antisymmetrized Hall resistivity as a function of the magnetic field at various temperatures [see Figs. S6(a) and S6(b) in the Supplemental Material for the measured magnetoresistivities [42]]. The reason we symmetrized and antisymmetrized the data is that a temperature-independent crossing point ( $B = 0.97$  T) was observed in the temperature range 0.5–1.5 K. For  $T > 1.5$  K, a deviation from a clear  $T$ -independent point of the 0–6 transition appears as  $T$  was further increased, consistent with previous work [53]. For  $B < 0.97$  T, we observed an insulating behavior in which the longitudinal resistivity decreased with increasing temperature. On the other hand, for  $B > 0.97$  T, the longitudinal resistivity decreased as the temperature decreased. Additionally, at higher magnetic fields, the longitudinal resistivity exhibited a local minimum, and the Hall resistivity approached a quantized value of  $h/(6e^2)$ . Although the  $\nu = 6$  quantum Hall plateau was not well developed, the presence of such a crossing point might indicate a transition from an insulating state to a  $\nu = 6$  quantum Hall state [this direct insulator to quantum Hall transition is further demonstrated from the temperature dependence of longitudinal resistivity under different magnetic fields shown in Fig. S7(a) of the Supplemental Material [42]].

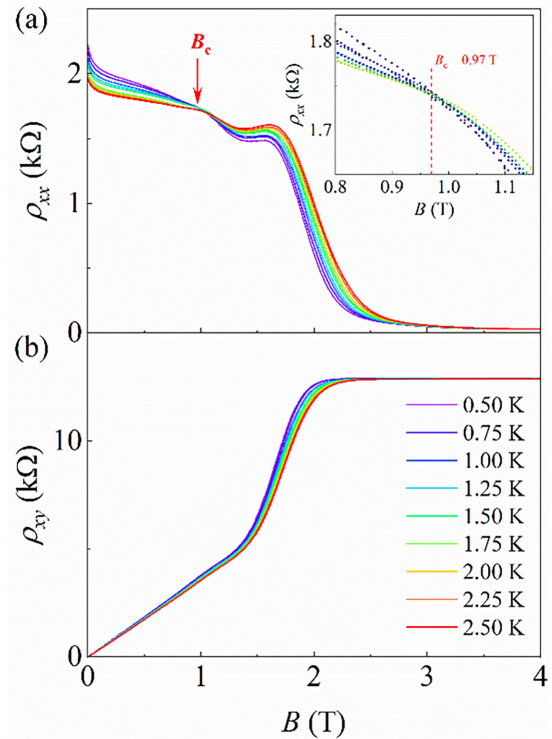


FIG. 1. Magnetotransport measurements before illumination. (a) The longitudinal resistivity and (b) Hall resistivity as a function of magnetic field at various temperatures. In  $\rho_{xx}$ , a temperature-independent crossing point ( $B = 0.97$  T) is observed within the temperature range 0.5–1.5 K.

In order to further study the observed direct I-QH transition from an insulator to a  $\nu = 6$  quantum Hall state, the graphene device was illuminated by an infrared light emitting diode (IR LED) so as to increase its carrier density (see Fig. S9 in the Supplemental Material for the spectrum of the IR LED [42] (see also references [54] therein)). After illumination, the carrier density of the device increased from  $n = 1.77 \times 10^{11} \text{ cm}^{-2}$  to  $n = 2.73 \times 10^{11} \text{ cm}^{-2}$ , while the mobility decreased from  $\mu = 15900 \text{ cm}^2 \text{ V}^{-1} \text{ s}^{-1}$  to  $\mu = 3200 \text{ cm}^2 \text{ V}^{-1} \text{ s}^{-1}$ . This effect exhibited a saturation behavior within a few seconds. Importantly, the effect induced by the illumination could be retained for an extended period, up to at least a few days, at temperatures below 30 K. This allowed for stable and reproducible measurements of the transport properties of the graphene device over an extended period of time. As shown in Fig. 2, the measurements were conducted at various temperatures ranging 0.5 to 30 K, and a clear and temperature-independent crossing point was observed in the longitudinal resistivity (at  $B_c = 1.13$  T) within the low-temperature range 0.5–2.0 K, indicating the presence of a quantum phase transition [53,55] [see Figs. S6(c) and S6(d) of the Supplemental Material for the measured magnetoresistivities [42]]. Moreover, the  $\nu = 6$  quantum Hall plateau had become more discernible. These observations provide clear evidence for a direct I-QH transition corresponding to an insulator to  $\nu = 6$  transition [the temperature dependence of longitudinal resistivity under different magnetic fields is shown in Fig. S7(b) of the Supplemental Material [42]].

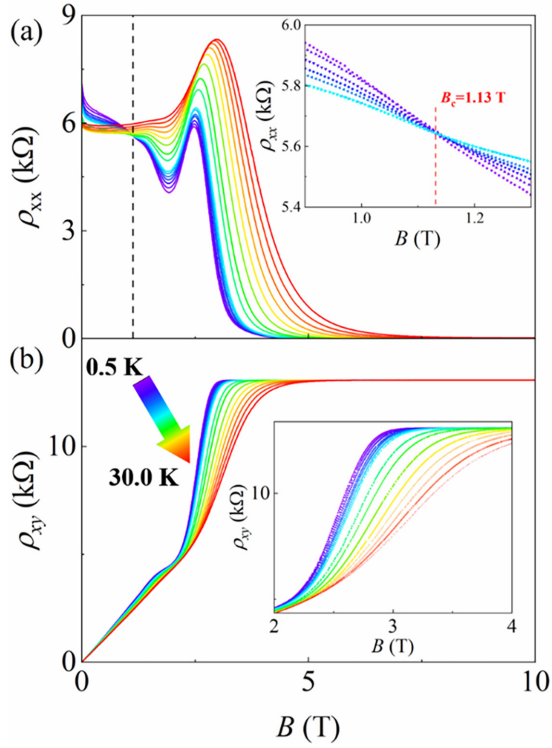


FIG. 2. Magnetotransport measurements after illumination. The symmetrized longitudinal resistivity and antisymmetrized Hall resistivity plotted as a function of magnetic field at various temperatures. (a) The inset highlights a clear crossing point at  $B_c = 1.13$  T, separating the insulating state and the  $\nu = 6$  quantum Hall state. (b) The inset shows the quantum critical regime of P-P transition.

Furthermore, a fully quantized  $\nu = 2$  quantum Hall plateau was developed with vanishing longitudinal resistivity and a quantized Hall resistivity  $h/(2e^2)$ . This provides an opportunity to investigate the P-P transition from a  $\nu = 6$  to a  $\nu = 2$  QH state.

*Scaling analysis of the direct I-QH transition and P-P transition.* To examine the scaling behavior of the direct I-QH transition and the P-P transition, a scaling analysis

was performed. The temperature-independent point, which characterized the I-QH transition, provided the basis for analyzing the data using the scaling theory of the quantum Hall effect. The scaling relation near the critical magnetic field was investigated, and it was found to follow the equation  $|\partial\rho_{xx}/\partial B|_{B=B_c} \sim T^{-\kappa}$ . By performing a linear fit on the data shown in Fig. 3(a), the critical exponent  $\kappa$  was determined to be  $0.41 \pm 0.02$  for the direct I-QH transition. To further illustrate the universal scaling behavior, the one-parameter scaling relation  $\rho_{xx} = f[|B - B_c|T^{-\kappa}]$  was plotted in the inset of Fig. 3(a). Readers interested in the scaling analysis performed at lower carrier densities are directed to Supplemental Material Sec. 6 [42]. Near the transition point, it was observed that all curves collapsed into two branches, which exhibited symmetry with respect to the transition point. This scaling analysis provides valuable insight into the behavior of the direct I-QH transition and demonstrates its universality.

On the other hand, between two adjacent quantum Hall plateaux, we also examine the maximum slope of  $\rho_{xy}$ , denoted as  $(|\partial\rho_{xy}/\partial B|^{\max})$ , which exhibited a temperature-dependent power law as  $|\partial\rho_{xy}/\partial B|^{\max} \sim T^{-\kappa}$ . As shown in Fig. 3(b), the linear fit of  $\ln|\partial\rho_{xy}/\partial B|^{\max} - \ln T$  in the high temperature region yielded a critical exponent  $\kappa = 0.42 \pm 0.02$  for the  $\nu = 6$  to  $\nu = 2$  quantum Hall P-P transition. It is important to point out that the saturation of the critical exponent at low temperatures can be attributed to finite-size effects [22,24–26]. As the temperature decreases, the coherence length  $\xi$  increases as temperature following the power law of  $\xi \sim T^{-p/2}$  where  $p$  is the temperature exponent. When the temperature becomes sufficiently low, the coherence length  $\xi$  can reach a comparable magnitude to the intrinsic characteristic length of the graphene. At this point, the dominant length scale shifts from the coherence length  $\xi$  to intrinsic length of graphene, resulting in the observed saturation behavior. To validate the saturation of the coherence length, a weak-localization (WL) analysis was performed, and the corresponding values of coherence length  $\xi$  were obtained. These results will be presented and discussed in the subsequent section, providing further evidence for the saturation of the coherence length.

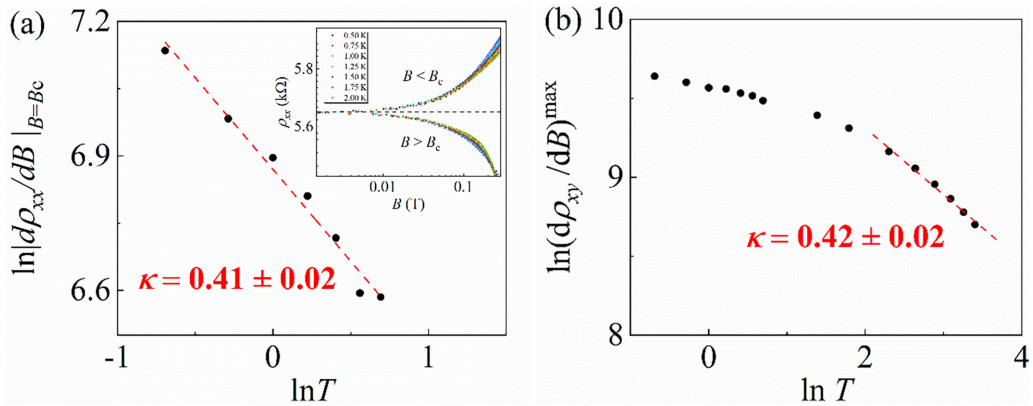


FIG. 3. Scaling behavior and critical exponents in the quantum critical regime. The solid circles represent the experimental data, and the dashed red line corresponds to the linear fit, providing the critical exponent  $\kappa$ . (a)  $\ln|\partial\rho_{xx}/\partial B|_{B=B_c}$  versus  $\ln T$  for the direct I-QH transition. The inset in (a) shows the one-parameter relation, where all curves collapse into a single curve near the critical magnetic field. (b)  $\ln|\partial\rho_{xy}/\partial B|^{\max}$  versus  $\ln T$  for the  $\nu = 6-2$  transition.

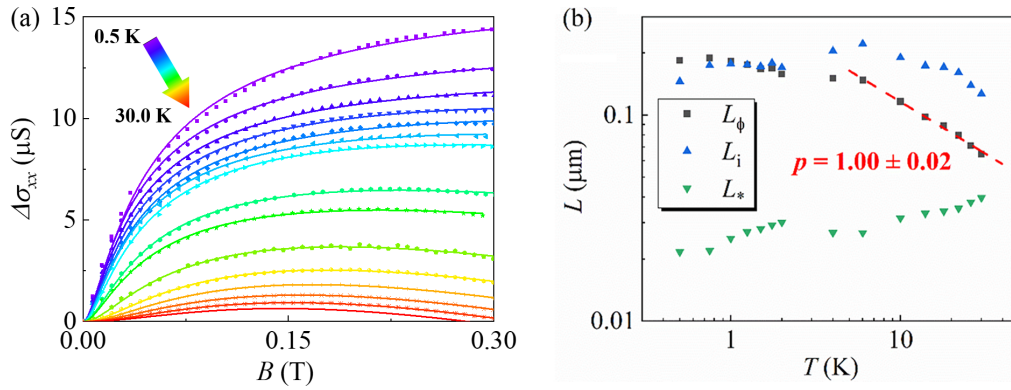


FIG. 4. Estimation of the coherence length  $L_\phi$  and temperature exponent  $p$ . (a) The converted magnetoconductivity plotted as a function of magnetic field. The solid symbols represent the experimental data, and the solid curves represent the best fits to Eq. (1). (b) The temperature dependence of the characteristic lengths plotted on a log-log scale. By utilizing the relation  $L_\phi \sim T^{-p/2}$ , the temperature exponent  $p$  was determined through a linear fit in the high-temperature region.

*Weak-localization effect and estimation of the temperature exponent.* In an effort to further study the scaling behavior, we examined the localization length by analyzing the WL effect in the low field region. This analysis allowed us to determine the coherence length and obtain the temperature exponent  $p$ . The magnetoconductivity difference, defined as  $\Delta\sigma_{xx} = \sigma_{xx}(B) - \sigma_{xx}(B=0)$ , was plotted as a function of magnetic field, as shown in Fig. 4(a). We analyzed the data using the expression derived by McCann *et al.* [56],

$$\Delta\sigma_{xx}(B) = \frac{e^2}{\pi h} \left[ F\left(\frac{8\pi B}{eL_\phi^{-2}}\right) - F\left(\frac{8\pi B}{\frac{h}{e}(L_\phi^{-2} + 2L_i^{-2})}\right) - 2F\left(\frac{8\pi B}{\frac{h}{e}(L_\phi^{-2} + L_i^{-2} + L_*^{-2})}\right) \right]. \quad (1)$$

Here,  $F(z) = \ln z + \psi(\frac{1}{2} + z^{-1})$ ,  $\psi(x)$  is the digamma function,  $L_\phi$  is the coherence length,  $L_i$  and  $L_*$  represent the characteristic scattering lengths for intervalley scattering and intravalley scattering process, respectively. These characteristic scattering lengths are extracted from Eq. (1) and displayed in Fig. 4(b). According to the relation  $L_\phi \sim T^{-p/2}$ , the temperature exponent  $p$  is determined to be  $1.00 \pm 0.02$  from the linear fit in the high-temperature region depicted in Fig. 4(b). The saturation observed at low temperatures can be attributed to factors such as self-heating or intrinsic scattering length [57]. It is worth mentioning that previous studies on monolayer [57,58] and bilayer [59] graphene have reported a similar value of approximately  $p = 1$  for the temperature exponent  $p$ . However, for epitaxial graphene, a study indicates that the value of  $p$  varies between 1 and 2 depending on the specific sample [60].

To further enhance our understanding of the scaling behavior, we calculated the universal exponent  $\gamma$  using the relationship  $\gamma = p/2\kappa$ , and the obtained value  $\gamma$  was found to be  $1.22 \pm 0.13$ . It is worth noting that the universal value could approximately be the value of 2.4 [61,62] or 4/3 [63–65], which is predicted by theoretical calculations based on quantum percolation or classical percolation, respectively. The value of  $1.22 \pm 0.13$ , which is close to 4/3, might indicate that the classical percolation dominates the scaling behavior in our sample.

*Discussion and conclusion.* Our experimental findings provide evidence for a direct I-QH transition to the  $\nu = 6$  QH state, which cannot be explained by the GPD [2]. Importantly, the presence of a well-defined temperature-independent crossing point and collapse of data into two branches near the crossing point indicate that this direct I-QH transition is a genuine phase transition rather than a broad crossover from localization to Landau quantization [10,66].

Different from the previous reports on the direct I-QH transition in various quasi-2D systems [3–15], the observation of the direct I-QH transition in monolayer graphene, which is truly a 2D system, is particularly exciting. Furthermore, the coexistence of the I-QH transition and the P-P transition within a single device provides an excellent opportunity to investigate whether these two transitions are of the same universality class. By studying their critical exponents, we can determine if they share a similar scaling behavior and underlying physics. This comparative analysis will contribute to our understanding of the fundamental nature of these transitions and their manifestation in different systems. The critical exponent  $\kappa$ , which characterizes the behavior near the transition, holds valuable insights into the system's properties [18–20]. Remarkably, in the case of monolayer graphene, a purely 2D system with Dirac fermions, the critical exponent  $\kappa \approx 0.42$  obtained from the direct I-QH transition displays a strong consistency with the value determined from the P-P transition.

Finally, we discuss the similarities and differences between the direct I-QH transition in monolayer graphene and those observed in conventional heterostructure-based 2D charge carriers [1,6,8–10,12,13,15]. Similar to its conventional 2D counterparts, there are two branches of data sets which obey scaling behavior in the vicinity of the direct I-QH transition in monolayer graphene, suggesting that the direct I-QH transition is a genuine quantum phase transition [4,8,9]. Moreover, both spin and valley degeneracies play an important role in the direct I-QH transition observed in conventional 2D charge systems [1,4,8,9] as well as in monolayer graphene. The Berry phase exists and anomalous integer quantum Hall effect (both unique for monolayer graphene but are not present in conventional 2D charge systems) occurs for Landau level filling factors  $\nu = 4(n + 1/2)$ , where  $n = 0, 1, 2, \dots$ . Therefore, for

monolayer graphene, the highest Landau level filling factor for which the direct I-QH transition can occur is  $\nu = 6$ , instead of 3 as clearly observed in the seminal work of Song and co-workers [1]. In some spin-degenerate charge systems, which show the direct I-QH transition, the critical exponent  $\kappa$  is close to  $0.42/(\text{spin degeneracy} = 2) = 0.21$  [6,8]. However, in monolayer graphene,  $\kappa$  is close to 0.41 [23,25] which deviates a lot from  $0.42/(\text{spin and valley degeneracies} = 4) = 0.105$ . The aforementioned differences between the direct I-QH transition in graphene and those in conventional 2D charge systems warrant further investigation.

In conclusion, we have observed the coexistence of the direct I-QH ( $0-\nu = 6$ ) transition and the quantum Hall P-P ( $\nu = 6$  to  $\nu = 2$ ) transition in monolayer epitaxial graphene. This observation, in a truly 2D system, offers unique insights. The distinct scaling properties near the critical magnetic field emphasize the genuine phase nature of the direct I-QH transition. Further, our scaling analysis places the direct I-QH transition and the P-P transition within the same universality class, with critical exponents  $\kappa$  being  $0.41 \pm 0.02$  and  $0.42 \pm 0.02$ , respectively. These discernments pave the way for a deeper understanding of the direct I-QH transition in two dimensions.

*Acknowledgments.* We acknowledge support by the Ministry of Science and Technology (MOST) and National Science and Technology Council (NSTC), Taiwan for finan-

cial support (Grants No. MOST 110-2112-M-002-029 -MY3, No. NSTC 111-2627-M-002-001, No. NSTC 111-2119-M-002-007, and No. NSTC 112-2119-M-002-014). We thank Prof. S.-T. Lo for helpful discussion and W.-R. Syong for experimental help. Additionally, the authors would like to express thanks to N. T. M. Tran, F. Fei, G. J. Fitzpatrick, and E. C. Benck for their assistance in the NIST internal review process.

Commercial equipment, instruments, and materials are identified in this paper in order to specify the experimental procedure adequately. Such identification is not intended to imply recommendation or endorsement by the National Institute of Standards and Technology or the United States Government, nor is it intended to imply that the materials or equipment identified are necessarily the best available for the purpose.

C.-C.Y. and P.-C.L. performed the transport measurement. D.K.P. grew the graphene films, fabricated the device, and performed sample characterization with the help of A.F.R. and R.E.E. C.-C.Y. and S.-C.W. analyzed the data. C.-C.Y., W.-C.L., and C.-T.L. wrote the manuscript with contributions from all authors. C.-T.L. conceived and supervised the project.

The authors declare that they have no known competing financial interests or personal relationships that could have appeared to influence the work reported in this paper.

- 
- [1] S.-H. Song, D. Shahar, D. C. Tsui, Y. H. Xie, and D. Monroe, New universality at the magnetic field driven insulator to integer quantum Hall effect transitions, *Phys. Rev. Lett.* **78**, 2200 (1997).
- [2] S. Kivelson, D.-H. Lee, and S.-C. Zhang, Global phase diagram in the quantum Hall effect, *Phys. Rev. B* **46**, 2223 (1992).
- [3] H. W. Jiang, C. E. Johnson, K. L. Wang, and S. T. Hannahs, Observation of magnetic-field-induced delocalization: Transition from Anderson insulator to quantum Hall conductor, *Phys. Rev. Lett.* **71**, 1439 (1993).
- [4] T. Wang, K. P. Clark, G. F. Spencer, A. M. Mack, and W. P. Kirk, Magnetic-field-induced metal-insulator transition in two dimensions, *Phys. Rev. Lett.* **72**, 709 (1994).
- [5] R. J. F. Hughes, J. T. Nicholls, J. E. F. Frost, E. H. Linfield, M. Pepper, C. J. B. Ford, D. A. Ritchie, G. A. C. Jones, E. Kogan, and M. Kaveh, Magnetic-field-induced insulator-quantum Hall-insulator transition in a disordered two-dimensional electron gas, *J. Phys.: Condens. Matter* **6**, 4763 (1994).
- [6] C. H. Lee, Y. H. Chang, Y. W. Suen, and H. H. Lin, Magnetic-field-induced delocalization in center-doped GaAs/Al<sub>x</sub>Ga<sub>1-x</sub>As multiple quantum wells, *Phys. Rev. B* **58**, 10629 (1998).
- [7] I. P. Smorchkova, N. Samarth, J. M. Kikkawa, and D. D. Awschalom, Giant magnetoresistance and quantum phase transitions in strongly localized magnetic two-dimensional electron gases, *Phys. Rev. B* **58**, R4238 (1998).
- [8] C. F. Huang, Y. H. Chang, C. H. Lee, H. T. Chou, H. D. Yeh, C.-T. Liang, Y. F. Chen, H. H. Lin, H. H. Cheng, and G. J. Hwang, Insulator-quantum Hall conductor transitions at low magnetic field, *Phys. Rev. B* **65**, 045303 (2001).
- [9] K. H. Gao, G. Yu, Y. M. Zhou, L. M. Wei, T. Lin, L. Y. Shang, L. Sun, R. Yang, W. Z. Zhou, N. Dai, J. H. Chu, D. G. Austing, Y. Gu, and Y. G. Zhang, Insulator-quantum Hall conductor transition in high electron density gated InGaAs/InAlAs quantum wells, *J. Appl. Phys.* **108**, 063701 (2010).
- [10] C.-T. Liang and S.-T. Lo, The direct insulator-quantum Hall transition. Chin, *J. Phys.* **52**, 1175 (2014).
- [11] C. F. Huang, Y. H. Chang, H. H. Cheng, C.-T. Liang, and G. J. Hwang, A study on the universality of the magnetic-field-induced phase transitions in the two-dimensional electron system in an AlGaAs/GaAs heterostructure, *Physica E* **22**, 232 (2004).
- [12] C.-T. Liang, L.-H. Lin, C. K. Yang, S.-T. Lo, Y.-T. Wang, D.-S. Lou, G.-H. Kim, Y.-H. Chang, Y. Ochiai, N. Aoki, J.-C. Chen, Y. Lin, C.-F. Huang, S.-Di. Lin, and D. A. Ritchie, On the direct insulator-quantum Hall transition in two-dimensional electron systems in the vicinity of nanoscaled scatterers, *Nanoscale. Res. Lett.* **6**, 131 (2011).
- [13] T.-Y. Huang, C.-T. Liang, G.-H. Kim, C. F. Huang, C.-P. Huang, J.-Y. Lin, H.-S. Goan, and D. A. Ritchie, From insulator to quantum Hall liquid at low magnetic fields, *Phys. Rev. B* **78**, 113305 (2008).
- [14] S.-T. Lo, Y.-T. Wang, S.-D. Lin, G. Strasser, J. P. Bird, Y.-F. Chen, and C.-T. Liang, Tunable insulator-quantum Hall transition in a weakly interacting two-dimensional electron system, *Nanoscale. Res. Lett.* **8**, 307 (2013).
- [15] K. Y. Chen, Y. H. Chang, C.-T. Liang, N. Aoki, Y. Ochiai, C. F. Huang, L.-H. Lin, K. A. Cheng, H. H. Cheng, H. H. Lin, J.-Y. Wu, and S.-D. Lin, Probing Landau quantization with the presence of insulator-quantum Hall transition in a GaAs

- two-dimensional electron system, *J. Phys.: Condens. Matter* **20**, 295223 (2008).
- [16] E. Pallecchi, M. Ridene, D. Kazazis, F. Lafont, F. Schopfer, W. Poirier, M. O. Goerbig, D. Mailly, and A. Ouerghi, Insulating to relativistic quantum Hall transition in disordered graphene, *Sci. Rep.* **3**, 1791 (2013).
- [17] L.-I. Huang, Y. Yang, R. E. Elmquist, S.-T. Lo, F.-H. Liu, and C.-T. Liang, Insulator-quantum Hall transition in monolayer epitaxial graphene, *RSC Adv.* **6**, 71977 (2016).
- [18] H. P. Wei, D. C. Tsui, M. A. Paalanen, and A. M. M. Pruisken, Experiments on delocalization and universality in the integral quantum Hall effect, *Phys. Rev. Lett.* **61**, 1294 (1988).
- [19] A. M. M. Pruisken, Universal singularities in the integral quantum Hall effect, *Phys. Rev. Lett.* **61**, 1297 (1988).
- [20] S. W. Hwang, H. P. Wei, L. W. Engel, D. C. Tsui, and A. M. M. Pruisken, Scaling in spin-degenerate Landau levels in the integer quantum Hall effect, *Phys. Rev. B* **48**, 11416 (1993).
- [21] S. Koch, R. J. Haug, K. v. Klitzing, and K. Ploog, Direct measurement of critical exponents in the quantum Hall regime, *Surf. Sci.* **263**, 108 (1992).
- [22] B. Huckestein, Scaling theory of the integer quantum Hall effect, *Rev. Mod. Phys.* **67**, 357 (1995).
- [23] A. J. M. Giesbers, U. Zeitler, L. A. Ponomarenko, R. Yang, K. S. Novoselov, A. K. Geim, and J. C. Maan, Scaling of the quantum Hall plateau-plateau transition in graphene, *Phys. Rev. B* **80**, 241411(R) (2009).
- [24] W. Li, C. L. Vicente, J. S. Xia, W. Pan, D. C. Tsui, L. N. Pfeiffer, and K. W. West, Scaling in Plateau-to-Plateau Transition: A direct connection of quantum Hall systems with the Anderson localization model, *Phys. Rev. Lett.* **102**, 216801 (2009).
- [25] T. Shen, A. T. Neal, M. L. Bolen, J. J. Gu, L. W. Engel, M. A. Capano, and P. D. Ye, Quantum-Hall plateau plateau transition in top-gated epitaxial graphene grown on SiC (0001), *J. Appl. Phys.* **111**, 013716 (2012).
- [26] X. Wang, H. Liu, J. Zhu, P. Shan, P. Wang, H. Fu, L. Du, L. N. Pfeiffer, K. W. West, X. C. Xie, R.-R. Du, and X. Lin, Scaling properties of the plateau transitions in the two-dimensional hole gas system, *Phys. Rev. B* **93**, 075307 (2016).
- [27] C.-C. Yeh, S.-C. Wang, S.-T. Lo, G.-H. Kim, D. A. Ritchie, G. Strasser, and C.-T. Liang, Quantum Hall plateau-plateau transition revisited, *Chin. J. Phys.* **82**, 149 (2023).
- [28] X. Kou, L. Pan, J. Wang, Y. Fan, E. S. Choi, W.-L. Lee, T. Nie, K. Murata, Q. Shao, S.-C. Zhang, and K. L. Wang, Metal-to-insulator switching in quantum anomalous Hall states, *Nat. Commun.* **6**, 8474 (2015).
- [29] P. Deng, C. Eckberg, P. Zhang, G. Qiu, E. Emmanouilidou, G. Yin, S. K. Chong, L. Tai, N. Ni, and K. L. Wang, Probing the mesoscopic size limit of quantum anomalous Hall insulators, *Nat. Commun.* **13**, 4246 (2022).
- [30] X. Wu, D. Xiao, C.-Z. Chen, J. Sun, L. Zhang, M. H. W. Chan, N. Samarth, X. C. Xie, X. Lin, and C.-Z. Chang, Scaling behaviour of the quantum phase transition from a quantum-anomalous-Hall insulator to an axion insulator, *Nat. Commun.* **11**, 4532 (2020).
- [31] V. P. Gusynin and S. G. Sharapov, Unconventional integer quantum Hall effect in graphene, *Phys. Rev. Lett.* **95**, 146801 (2005).
- [32] S. Koch, R. J. Haug, K. v. Klitzing, and K. Ploog, Experiments on scaling in  $\text{Al}_x\text{Ga}_{1-x}\text{As}/\text{GaAs}$  heterostructures under quantum Hall conditions, *Phys. Rev. B* **43**, 6828 (1991).
- [33] W. Li, G. A. Csáthy, D. C. Tsui, L. N. Pfeiffer, and K. W. West, Scaling and universality of integer quantum Hall plateau-to-plateau transitions, *Phys. Rev. Lett.* **94**, 206807 (2005).
- [34] S. Koch, R. J. Haug, K. v. Klitzing, and K. Ploog, Size-dependent analysis of the metal-insulator transition in the integral quantum Hall effect, *Phys. Rev. Lett.* **67**, 883 (1991).
- [35] S. Koch, R. J. Haug, K. v. Klitzing, and K. Ploog, Experimental studies of the localization transition in the quantum Hall regime, *Phys. Rev. B* **46**, 1596 (1992).
- [36] M. Kruskopf, A. F. Rigosi, A. R. Panna, M. Marzano, D. Patel, H. Jin, D. B. Newell, and R. E. Elmquist, Next-generation crossover-free quantum Hall arrays with superconducting interconnections, *Metrologia* **56**, 065002 (2019).
- [37] A. F. Rigosi, M. Kruskopf, H. M. Hill, H. Jin, B.-Y. Wu, P. E. Johnson, S. Zhang, M. Berilla, A. R. H. Walker, C. A. Hacker, D. B. Newell, and R. E. Elmquist, Gateless and reversible Carrier density tunability in epitaxial graphene devices functionalized with chromium tricarbonyl, *Carbon* **142**, 468 (2019).
- [38] S. M. Mhatre, N. T. M. Tran, H. M. Hill, D. Saha, A. R. H. Walker, C.-T. Liang, R. E. Elmquist, D. B. Newell, and A. F. Rigosi, Dynamics of transient hole doping in epitaxial graphene, *Phys. Rev. B* **105**, 205423 (2022).
- [39] S. M. Mhatre, N. T. M. Tran, H. M. Hill, C.-C. Yeh, D. Saha, D. B. Newell, A. R. Hight Walker, C.-T. Liang, R. E. Elmquist, and A. F. Rigosi, Versatility of uniformly doped graphene quantum Hall arrays in series, *AIP Adv.* **12**, 085113 (2022).
- [40] D. G. Jarrett, C.-C. Yeh, S. U. Payagala, A. R. Panna, Y. Yang, L. Meng, S. M. Mhatre, N. T. M. Tran, H. M. Hill, D. Saha, R. E. Elmquist, D. B. Newell, and A. F. Rigosi, Graphene-based Star–Mesh resistance networks, *IEEE Trans. Instrum. Meas.* **72**, 1 (2023).
- [41] A. R. Panna, I.-F. Hu, M. Kruskopf, D. K. Patel, D. G. Jarrett, C.-I. Liu, S. U. Payagala, D. Saha, A. F. Rigosi, D. B. Newell, C.-T. Liang, and R. E. Elmquist, Graphene quantum Hall effect parallel resistance arrays, *Phys. Rev. B* **103**, 075408 (2021).
- [42] See Supplemental Material at <http://link.aps.org/supplemental/10.1103/PhysRevB.108.205304> for details on epitaxial growth, graphene characterization, fabrication process, and measured results, which includes Refs. [43–49].
- [43] M. A. Real, E. A. Lass, F.-H. Liu, T. Shen, G. R. Jones, J. A. Soons, D. B. Newell, A. V. Davydov, and R. E. Elmquist, Graphene Epitaxial growth on SiC(0001) for resistance standards, *IEEE Trans. Instrum. Meas.* **62**, 1454 (2013).
- [44] Y. Yang, G. Cheng, P. Mende, I. G. Calizo, R. M. Feenstra, C. Chuang, C.-W. Liu, C.-I. Liu, G. R. Jones, A. R. H. Walker, and R. E. Elmquist, Epitaxial graphene homogeneity and quantum Hall effect in millimeter-scale devices, *Carbon* **115**, 229 (2016).
- [45] M. Kruskopf, D. M. Pakdehi, K. Pierz, S. Wunderack, R. Stosch, T. Dziomba, M. Götz, J. Baringhaus, J. Aprojanz, C. Tegenkamp, J. Lidzba, T. Seyller, F. Hohls, F. J. Ahlers, and H. W. Schumacher, Comeback of epitaxial graphene for electronics: Large-area growth of bilayer-free graphene on SiC, *2D Mater.* **3**, 041002 (2016).
- [46] V. Panchal, Y. Yang, G. Cheng, J. Hu, M. Kruskopf, C.-I. Liu, A. F. Rigosi, C. Melios, A. R. H. Walker, D. B. Newell, O. Kazakova, and R. E. Elmquist, Confocal laser scanning microscopy for rapid optical characterization of graphene, *Commun. Phys.* **1**, 83 (2018).
- [47] D. M. Pakdehi, K. Pierz, S. Wunderack, J. Aprojanz, T. T. N. Nguyen, T. Dziomba, F. Hohls, A. Bakin, R. Stosch, C.

- Tegenkamp, F. J. Ahlers, and H. W. Schumacher, Minimum resistance anisotropy of epitaxial graphene on SiC, *ACS Appl. Mater. Interfaces* **10**, 6039 (2018).
- [48] M. Büttiker, Four-terminal phase-coherent conductance, *Phys. Rev. Lett.* **57**, 1761 (1986).
- [49] H. H. Sample, W. J. Bruno, S. B. Sample, and E. K. Sichel, Reverse-field reciprocity for conducting specimens in magnetic fields, *J. Appl. Phys.* **61**, 1079 (1987).
- [50] M. Büttiker, Symmetry of electrical conduction, *IBM J. Res. Dev.* **32**, 317 (1988).
- [51] M. Hilke, D. Shahar, S. H. Song, D. C. Tsui, Y. H. Xie, and Don Monroe, Experimental evidence for a two-dimensional quantized Hall insulator, *Nature (London)* **395**, 675 (1998).
- [52] C. Li, B. D. Ronde, A. Nikitin, Y. Huang, M. S. Golden, A. d. Visser, and A. Brinkman, Interaction between counter-propagating quantum Hall edge channels in the 3D topological insulator BiSbTeSe<sub>2</sub>, *Phys. Rev. B* **96**, 195427 (2017).
- [53] C. F. Huang, Y. H. Chang, H. H. Cheng, Z. P. Yang, S. Y. Wang, H. D. Yeh, H. T. Chou, C. P. Lee, and G. J. Hwang, On the equivalence between magnetic-field-induced phase transitions in the integer quantum Hall effect, *Solid State Commun.* **126**, 197 (2003).
- [54] S. Rathore, D. K. Patel, M. K. Thakur, G. Haider, M. Kalbac, M. Kruskopf, C.-I. Liu, A. F. Rigosi, R. E. Elmquist, C.-T. Liang, and P.-D. Hong, Highly sensitive broadband binary photore-sponse in gateless epitaxial graphene on 4H-SiC, *Carbon* **184**, 72 (2021).
- [55] C.-T. Liang, C. F. Huang, Y.-M. Cheng, T.-Y. Huang, Y. H. Chang, and Y. F. Chen, Studies of the temperature-driven flow lines and phase transitions in a two-dimensional Si/SiGe hole system, *Chin. J. Phys.* **39**, L305 (2001).
- [56] E. McCann, K. Kechedzhi, V. I. Fal'ko, H. Suzuura, T. Ando, and B. L. Altshuler, Weak-localization magnetoresistance and valley symmetry in graphene, *Phys. Rev. Lett.* **97**, 146805 (2006).
- [57] F. V. Tikhonenko, D. W. Horsell, R. V. Gorbachev, and A. K. Savchenko, Weak localization in graphene flakes, *Phys. Rev. Lett.* **100**, 056802 (2008).
- [58] S. Pezzini, C. Cobaleda, E. Diez, and V. Bellani, Quantum interference corrections to magnetoconductivity in graphene, *Phys. Rev. B* **85**, 165451 (2012).
- [59] R. V. Gorbachev, F. V. Tikhonenko, A. S. Mayorov, D. W. Horsell, and A. K. Savchenko, Weak localization in bilayer graphene, *Phys. Rev. Lett.* **98**, 176805 (2007).
- [60] W. Pan, A. J. Ross, III, S. W. Howell, T. Ohta, T. A. Friedmann, and C.-T. Liang, Electron-electron interaction in high-quality epitaxial graphene, *New J. Phys.* **13**, 113005 (2011).
- [61] J. T. Chalker and P. D. Coddington, Percolation, quantum tunnelling and the integer Hall effect, *J. Phys. C: Solid State Phys.* **21**, 2665 (1988).
- [62] B. Huckestein and B. Kramer, One-parameter scaling in the lowest Landau band: Precise determination of the critical behavior of the localization length, *Phys. Rev. Lett.* **64**, 1437 (1990).
- [63] D.-H. Lee, Z. Wang, and S. Kivelson, Quantum percolation and plateau transitions in the quantum Hall effect, *Phys. Rev. Lett.* **70**, 4130 (1993).
- [64] S. A. Trugman, Localization, percolation, and the quantum Hall effect, *Phys. Rev. B* **27**, 7539 (1983).
- [65] B. Kramer, T. Ohtsuki, and S. Kettemann, Random network models and quantum phase transitions in two dimensions, *Phys. Rep.* **417**, 211 (2005).
- [66] J.-H. Chen, J.-Y. Lin, J.-K. Tsai, H. Park, G.-H. Kim, J. Ahn, H.-I. Cho, E.-J. Lee, J.-H. Lee, C.-T. Liang, and Y. F. Chen, Experimental evidence for Drude-Boltzmann-like transport in a two-dimensional electron gas in an AlGaIn/GaN heterostructure, *J. Korean Phys. Soc.* **48**, 1539 (2006).